

Research Article

Risk Assessment of Rollover and Skidding due to Pavement Roughness and Differential Settlement for Enhancing Transportation Safety

Lu Sun ¹, Luchuan Chen,² Yanna Yin ³, Yao Tian,² and Xuanyu Zhang⁴

¹Rochester Institute of Technology, Rochester, New York, USA

²Shandong Expressway Co., Ltd., Jinan, China

³South China University of Technology, School of Civil Engineering and Transportation, No. 381 Wushan Road, Tianhe, Guangzhou 510006, China

⁴Shandong Expressway Infrastructure Construction Co., Ltd., Jinan, China

Correspondence should be addressed to Yanna Yin; 1241085280@qq.com

Received 22 August 2021; Accepted 9 November 2021; Published 9 December 2021

Academic Editor: Hocine Imine

Copyright © 2021 Lu Sun et al. This is an open access article distributed under the Creative Commons Attribution License, which permits unrestricted use, distribution, and reproduction in any medium, provided the original work is properly cited.

In this paper, a closed-loop simulation of vehicle dynamics in CarSim is utilized as surrogate measures to study the effect of pavement roughness and differential settlement on risk of vehicle rollover and skidding. It is found that the influence of pavement roughness on vehicle rollover is significant and the influence of pavement roughness on vehicle skidding is insignificant. The influence of pavement roughness of grade A and B on safety margin of vehicle rollover can be negligible. Pavement roughness of grade C and D significantly reduces the safety margin of vehicle rollover. A 5 cm settlement difference on pavement reduces the safety margin of vehicle skidding on a good road. When the settlement difference is 5 cm, the vehicle rollover and skidding are greatly affected by the lane-changing speed. It provides an effective and general method based on vehicle dynamics for studying transportation safety as well as for setting up criteria for pavement maintenance.

1. Introduction

Despite the decline in highway fatalities from 2001 to 2014 [1], the death toll caused by traffic accidents is still very high. Road safety has always been an issue of great concern to the public [2–5]. Traffic accidents are closely related to a number of factors: interaction among drivers, vehicles, roads, and road environments, such as road geometry, tire-road friction, speed, vehicle dynamics, vehicle performances, driver behaviors, and driving environments. Traditional road safety studies identify road sections with traffic accident and rely heavily on historical traffic accident data [6–9]. These methods belong to post hoc analysis and have limited usage for improving road safety for road during design stage.

Sun and his associates proposed a new method based on vehicle dynamics for road safety study [10–14]. The method analyzes dynamic responses of a vehicle model on a given

road considering road geometry (i.e., longitudinal, horizontal, and vertical alignments), pavement friction coefficient, operating speed of the road, pavement roughness [15–33], weather conditions, wind speed, driver behavior (i.e., lane-changing behavior), roadside environment, vehicle trajectory (i.e., lane-keeping and lane-departing), and other factors. The dynamic responses can be linked to traffic accident counts or percentage and therefore serve as excellent surrogate measures for evaluating road safety.

This vehicle-dynamics-based method has a number of advantages. First of all, it is objective and does not rely on the evaluator's subjective rating. Secondly, it is cost-effective and generally applicable to not only in-service roads but roads under design or construction, making it a proactive approach. Thirdly, it is flexible and fast and allows multiple factors encountered in real driving environment to be considered efficiently. This method has been used for

quantitatively assessing road safety in terms of rollover, skidding, and other types of accident for improving road geometry design, transportation operations management, road maintenance, and transportation safety [10–13].

Although vehicle rollover and skidding have been studied by many researchers, what is missing in literature is the study of pavement roughness and differential (longitudinal) settlement in pavement on vehicle rollover and skidding, which is the focus of this paper.

2. Literature Review

Vehicle's rollover is the main source of fatal traffic accidents. According to the New Mexico State Department of Transportation [34], the number of rollover accidents accounted for 5.2% of the total reported accidents in the U.S. and resulted in 34.6% of fatal accidents and 36.2% of the deaths of passengers. According to the National Highway Traffic Safety Administration (NHTSA), rollovers accidents in the United States accounted for 17.9% of all fatal accidents in 2016 [1]. Although the proportion of rollover accidents is not high, but the mortality rate in rollover accident is extremely high [35], along with huge economic losses.

Skidding seriously affects vehicle stability, which is another main contributing factor to traffic accidents. Studies have shown that lateral skidding typically (i.e., 66%) occurs before a vehicle rollover [8]. When a vehicle negotiates a horizontal alignment, the vehicle is prone to skidding if the operating speed of the vehicle is too high.

It is of great significance to study the causes of rollover and skidding. Based on the existing accident data, it is clear that road geometry, pavement friction coefficient, weather conditions, and driver behaviors contribute significantly to vehicle rollover and skidding [7, 9, 34, 36–39]. Farmer and Lund [40] studied the effects of road conditions (wet and dry), road alignment (curved and straight), road environment, and drivers on vehicle rollover and found that the probability of rollover in the dark was lower than that in the daytime, and the probability of rollover on wet road was lower than that on dry road. Hu and Donnell [41] studied the influence of vehicle, driver, roadway, and median cross section on rollover crash severity. Morgan and Mannering [7] studied single-vehicle crashes severities that occurred on dry, wet, and snow/ice-covered roadway surfaces, according to the database of single-vehicle crashes in Indiana in 2007 and 2008.

A few of researchers have studied vehicle rollover and skidding based on vehicle dynamics [10, 40–43]. Harwood and Mason [44] based on mass point model evaluated the margin of safety against vehicle skidding and rollover for both passenger cars and trucks traveling at the design speed. Lapapong and Brennan [45] carried out a dynamic analysis on vehicle rollover process and established a rollover risk state prediction model including superelevation, grade, shoulder, and other factors. Sun and You [10] comprehensively considered the influence of road geometry, road condition, roadside environment, etc., on vehicle rollover and skidding. You and Sun [11] analyzed the reliability of vehicle stability

on horizontal and vertical curves. The performance function based on mass model, vehicle dynamic simulation function considering skidding failure model, and vehicle dynamic simulation function considering rollover failure are proposed, respectively. Mavromatis et al. [46] determined the maximum attainable safe speed at impending skid conditions as well as the situation of comfortable curve negotiation where lower constant speed values were utilized.

Wang et al. [47]; Uys et al. [48]; and Kashyzadeh et al. [49] studied the influence of pavement roughness on vehicle vibration. Ma et al. [50] and Zhang et al. [51] studied the effect of pavement roughness on the root mean square value of weighted acceleration. Hu et al. [52] used two degrees of freedom vehicle model to study critical wind speed considering the effect of pavement roughness on vehicle rollover and skidding.

Highway and bridge widening are prevailing strategies to accommodate the growth of traffic volume [53–55]. A common practice of bridge widened is to splice a new bridge next to the existing bridge. The critical challenge of widening of old bridge is that the old bridge foundation has been stabilized at a level for many years, but the new bridge foundation will continue to settle in a few years after construction. The differential settlement will cause the height difference in pavement on new bridge and old bridges. When a vehicle makes lane change and crosses the differential settlement, the risk of skidding and rollover increases, posing a seriously threat to transportation safety.

Traffic accidents on bridges occur frequently. For example, on December 13, 2018, due to ponding freezes on the surface of Huaide Bridge in Changzhou of China, multi-vehicles collided caused by vehicle skidding [56]. On January 12, 2019, a SUV understeered and crashed into the central guardrail of the Hangzhou Bay Bridge. This SUV was rebounded and rolled over. The cause of this accident is that a car changed lane and collided with other vehicles [57]. On September 2, 2019, a collision accident of three vehicles occurred at Beihuan Overpass in Shenzhen, in which two vehicles overturned and fell to the auxiliary road [58].

A number of studies on traffic safety on bridge focus on the effect of lateral wind using vehicle dynamics. Fan [59] investigated traffic safety on bridge using vehicle dynamics simulation. Chen et al. [60] studied the influence of crosswind on vehicle driving safety of the part of a bridge connected to a tunnel through simulation test and selected yaw rate and steering angle as dynamic response indexes under crosswind. Zhou and Chen [61] accurately obtained the dynamic response of each vehicle in random traffic by considering the full coupling effect of traffic flow, bridge, wind, and other vehicles. Pan et al. [62], based on the wind-vehicle-bridge theory, established a driving simulation of experiment scene of long-span bridges considering both crosswind and vibration. The influence of bridge vibration caused by lateral wind on the yaw angle of vehicle is studied. Yu et al. [63] took no skidding of vehicles as the index to set wind speed standard of the vehicle safety driving of cross sea bridge under different bridge floor characteristics.

3. Model of Vehicle Dynamics

CarSim is a multibody vehicle dynamics simulation software developed by UMTRI. The stability, reliability, and efficiency of CarSim have been tested by the automobile industry. CarSim simplifies vehicles into 10 parts: a vehicle body part, four unsprung mass parts, four rotating wheel parts, and an engine crankshaft part. The simplified model consists of 27 degrees of freedom for vehicle dynamics: three degrees of freedom of movement (x, y, z) of sprung mass, three degrees of freedom of rotation (x, y, z) of sprung mass, four degrees of freedom of unsprung mass, four degrees of freedom of wheel rotation, one degree of freedom of transmission system, eight degrees of freedom of tire transient characteristics, and four degrees of freedom of brake pressure.

There are two kinds of simulation systems for vehicle dynamics in CarSim: open-loop simulation and closed-loop simulation, as shown in Figure 1. The open-loop simulation system considers the vehicle as an independent control system. The system does not consider the driver's feedback. The closed-loop simulation system incorporates driver's feedback into the system. Drivers get information about the road ahead and vehicles through "preview" and "perception," and continuously correct the steering wheel angle by estimating the road condition. That is to say, the road condition is fed back to the driving state of the vehicle. Since the closed-loop system can more accurately reflect the driving state of a vehicle, it is adopted in this paper to study the effect of pavement roughness and pavement differential settlement on vehicle rollover and skidding.

Because SUV is more prone to rollover due to its higher center of gravity than that of passenger cars [36, 43, 64], SUV is adopted in this study as the model of vehicle to be studied. The driver model includes four parts: speed control, shift control, braking control, and steering control. In this paper, the fixed target speed control mode is adopted, and the closed-loop automatic shift control mode is selected. The steering control adopts the "1.5 s" forward-looking preview strategy. The road center line is considered as the vehicle target trajectory, and the vehicle is controlled to travel along the center line. Detailed parameters of the SUV model and the driver model can be found in authors' previous work [12, 13].

4. Safety Margins of Vehicle Rollover and Skidding

4.1. Safety Margin of Vehicle Rollover. There are two types of vehicle rollover, nontripped rollover and tripped rollover. When vehicles' lateral acceleration exceeds the compensation limit of lateral tire weight transfer, the vehicle rotates 90 degrees or more around its longitudinal axis, which is called nontripped rollover. Another is that when a vehicle slips, the vehicle loses control. The vehicle is impacted by superelevation, curb, mollisol, etc., so as to "trip" the vehicle and rotates 90 degrees or more around its longitudinal axis, which is called tripped rollover. Based on the above definition of nontripped rollover, lateral acceleration a_y is used to characterize vehicle nontripped rollover. Before tripped

rollover, the vehicle will generally skid. In this paper, tripped rollover is classified as skidding. Only nontripped rollover is studied, hereinafter referred to as rollover.

The quasistatic model of rigid vehicle [65] is shown in Figure 2 (ignoring the elastic deformation of the suspension and tire of the vehicle). The torque formula of quasistatic model of rigid vehicle is as follows. The moment reference point of moment balance is the contact point between the outside wheel on the roll plane and the ground:

$$(F \cos \beta - mg \sin \beta)h_g + N_{Zi} \cdot B - (F \sin \beta + mg \cos \beta) \cdot \frac{B}{2} = 0. \quad (1)$$

Here, F is the centrifugal force; α is the bank angle of the road; N_{yi} and N_{yo} are the lateral forces on the inner and outer tires, respectively; N_{Zi} and N_{Zo} are the vertical forces on the inner and outer tires, respectively; and B is the wheel-base.

According to Newton's second law, $F \cos \beta - mg \sin \beta = ma_y$, a_y is the lateral acceleration. Since the cross-slope angle β of the road is generally small, so $\sin \beta \approx \tan \beta = \beta = i_h$, $\cos \beta \approx 1$, which can be derived from equation (1) as follows:

$$ma_y h_g + F_{Zi} \cdot B - (F \beta + mg) \cdot \frac{B}{2} = 0. \quad (2)$$

When the lateral acceleration is large enough, the inner wheel will leave the ground. Namely, N_{Zi} is 0. The vehicle does not balance in the roll plane and begins to rollover. The lateral acceleration that the vehicle is at impending rollover conditions is called the rollover threshold, which can be derived from equation (2) as follows:

$$a_y = \frac{[F \beta + mg \cdot (B/2)]}{mh_g}. \quad (3)$$

In this paper, the minimum rollover threshold is used [65]. Namely, let $\beta = 0$; the rollover threshold of the rigid automobile is $a_y = B/2h_g g$. The parameters of SUV are substituted into the formula and get $a_y = 1.2g$. For SUV, the rollover threshold of physical model of roll is 30% lower than that of the quasistatic model of rigid vehicle [65]. Therefore, the threshold value of rollover here is $a_y^0 = 0.84$, and the corresponding rollover safety margin is as follows:

$$M_1 = a_y^0 - \max(|a_y(t)|) \quad 0 \leq M_1 \leq a_y^0. \quad (4)$$

4.2. Safety Margin of Vehicle Skidding. When a vehicle is traveling on a curve, the lateral force perpendicular to the direction of the vehicle will be produced due to the influence of centrifugal force and superelevation. When the lateral force is equal to or exceeds the maximum lateral adhesive force provided by the road surface, it will cause lateral slip of one or both axles of the vehicle, which is called skidding.

According to the definition of the skidding, the lateral force coefficient of wheels is used to characterize vehicle skidding in this paper. The lateral force coefficient formula of the vehicle is [65]

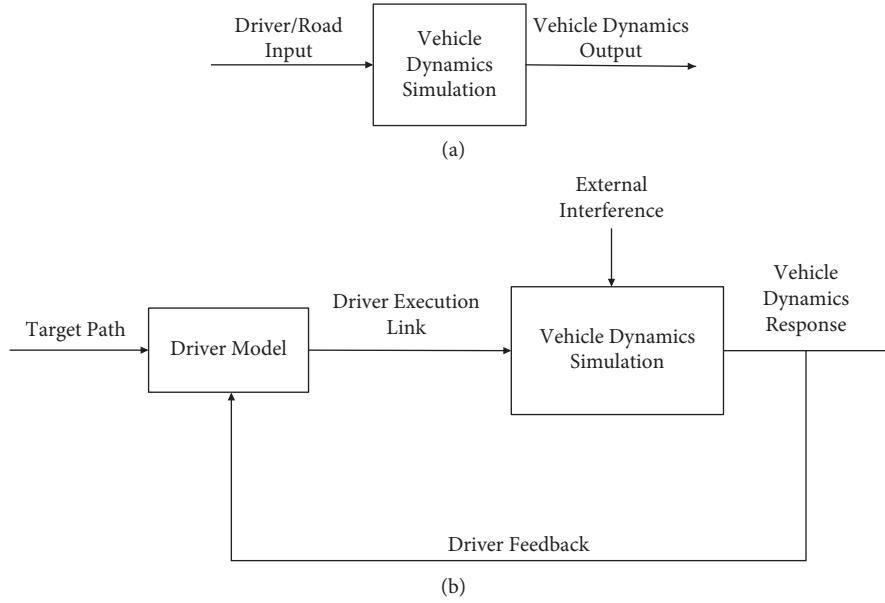


FIGURE 1: Flow chart of vehicle dynamics simulation. (a) Open-loop simulation. (b) Closed-loop simulation.

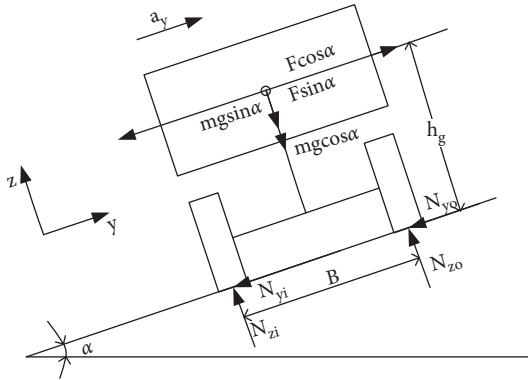


FIGURE 2: The quasistatic model of rigid vehicle.

$$\mu_l = \max\left(\left|\frac{F_{yi}}{F_{zi}}\right|\right), \quad i = 1, 2, 3, 4, \quad (5)$$

where F_{yi} is the tire lateral force; F_{zi} is the tire vertical force; and $i = 1, 2, 3, 4$ left-front wheel, left-rear wheel, right-front wheel, and right-rear wheel, respectively. When the lateral force coefficient of any wheel is greater than the maximum lateral road adhesion coefficient, the vehicle will skid. Let μ_l^0 be lateral force coefficient when the vehicle is at impending skid conditions. When $\mu_l > \mu_l^0$, skidding will occur. The road adhesion coefficients f_p studied here are 0.8, 0.5, and 0.2, corresponding to dry, wet, and snow conditions, respectively [65].

Road adhesion coefficient refers to the maximum longitudinal road adhesion coefficients. According to Lamm et al. [66], lateral maximum tire-road friction $f_{R\max} = 0.925 f_p$. However, a vehicle is at a high slip value in this paper; the brake is blocked or the slip is accelerated [67]. In such a situation, the maximum longitudinal friction coefficient is equivalent to the coefficient of sliding friction f_s .

Namely, $f_p = f_s$. Therefore, $f_{R\max} = 0.925 f_s$. Table 1 shows road adhesion coefficient, coefficient of sliding friction, and maximum lateral tire-road friction coefficient of asphalt on dry, wet, and snow pavements. Here, f_p is the road adhesion coefficient; f_s is the coefficient of sliding friction. Coefficient of sliding friction is equal to the braking force coefficient when the sliding rate is 100%, and $f_{R\max}$ is the lateral maximum tire-road friction coefficient.

The safety margin of vehicle skidding on a curve is defined as the difference between available tire-road (the lateral maximum tire-road friction coefficient provided) and the lateral friction demand [44]. So, the corresponding safety margin of vehicle skidding

$$M_2 = \mu_l^0 - \max(\mu_l) \quad 0 \leq M_2 \leq \mu_l^0. \quad (6)$$

5. Pavement Roughness

Road surface is a three-dimensional entity composed of horizontal curve, superelevation, and grade. Pavement roughness refers to the deviation value of the longitudinal concave convex amount of the road surface [68]. Pavement roughness is important for evaluating the microundulation and microgeometric dimension of road surface [69, 70]. In the cross section of the road, pavement roughness can be singularly manifested as rutting and cross section unevenness, which can cause vehicles to roll.

5.1. Pavement Roughness Classification. The international organization for standardization [71] first proposed the expression draft of road roughness. China's Changchun Automobile Research Institute formulated "pavement roughness representation" of the vehicle vibration input. Both documents adopt the power spectral density $G_q(n)$. The fitting expression of $G_q(n)$ is

TABLE 1: Pavement friction condition.

Road adhesion coefficient f_p	Coefficient of sliding friction f_s	Lateral maximum tire-road friction coefficient $f_{R\max} = 0.925f_s$
0.8	0.75	0.69
0.5	0.45	0.41
0.2	0.15	0.13

$$G_q(n_0) = G_q(n_0) \left(\frac{n}{n_0} \right)^{-\omega}, \quad (7)$$

where n is the spatial frequency and expresses the number of wavelengths per meter; n_0 is the reference spatial frequency $n_0 = 0.1\text{m}^{-1}$; $G_q(n_0)$ represents the coefficient of road roughness, which is road power spectral density value when the reference spatial frequency is n_0 (unit: $\text{m}^2/\text{m}^{-1} = \text{m}^3$); ω is the frequency index; and ω represents the slope of double logarithmic oblique line and reflects the structure of power spectral density of pavement. In the double logarithmic coordinates, (7) is a slant line. In order to reduce the fitting error in the actual measurement of pavement, different coefficients can be selected in the frequency range for piecewise fitting in different spaces.

ISO classifies pavement roughness into eight grades (ISO 2016), as shown in Table 2. This table also includes the corresponding coefficient $G_q(n_0)$ of pavement roughness of different grades and root mean square $q_{rms}(\sigma_q)$ corresponded to different grades of pavement roughness within the range $0.011\text{m}^{-1} < n < 2.83\text{m}^{-1}$.

5.2. Pavement Roughness Reconstruction. The common methods of road spectrum reconstruction include white noise method, Fourier transform method, time series model method, and harmonic superposition method. The filter structure of white noise method is not strict enough. Fourier transform method has strong expansibility, but compared with the harmonic superposition method, the accuracy is not enough. The simulation process of time series model method is long and the efficiency is low. Therefore, the harmonic superposition method is used in this paper. Although the computational burden of this method is heavy, the simulation accuracy is high.

In the method of harmonic superposition, the road signal is decomposed into a series of sine waves or cosine waves with different frequency and amplitude by discrete Fourier transform. The time domain or spatial domain model of pavement roughness can be obtained by superposition of a certain number or amount of harmonic waves. In this paper, sine wave is used to simulate random road surface. It is worth noting that great attention should be taken when artificial profiles of pavement are generated as presented in Loprencipe and Zoccali [72, 73] and Zoccali and Cantisani [74].

The power spectral density of pavement displacement is $G_q(n)$ in the space frequency of $0.011 < n < 2.83$, as shown in (7). In the stationary stochastic process, according to the expansion property of power spectral density, the pavement roughness variance σ_z^2 can be expressed as

$$\sigma_z^2 = \int_{n_1}^{n_2} G_q(n) dn. \quad (8)$$

Interval $[n_1, n_2]$ can be further divided into several intercells. The spectral density at the center frequency $n_{\text{mid-}i}$ ($i = 1, 2, \dots, k$) of each intercell $G_q(n_{\text{mid-}i})$ is used for replacing $G_q(n)$ of whole intercell. After discretization, the variance value of pavement roughness shown in formula (8) can be approximately expressed as follows:

$$\sigma_z^2 = \int_{n_1}^{n_2} G_q(n) dn. \quad (9)$$

Standard deviation of center frequency of each intercell is $\sqrt{G_q(n_{\text{mid-}i})n_i}$. The corresponding sine wave function is expressed as $\sqrt{2G_q(n_{\text{mid-}i})n_i} \sin(2\pi n_{\text{mid-}i}x + \theta_i)$. Therefore the sine wave function of different intercell is superimposed, the input value of random displacement space domain of pavement can be obtained as follows:

$$q(x) = \sum_{i=1}^n \sqrt{2G_q(n_{\text{mid-}i})\Delta n} \cdot \sin(2\pi n_{\text{mid-}i}x + \theta_i). \quad (10)$$

Here, $G_q(n_{\text{mid-}i})$ is the power spectral density (unit: $\text{m}^2/\text{m}^{-1} = \text{m}^3$); n is the frequency interval (unit: m^{-1}); X is the distance travelled (unit: m); and θ_i is a random variable between $[0, 2\pi]$, which is independent and uniformly distributed. When the interval is divided close enough, that is, when the k is very large, the frequency characteristics displayed by the random displacement input are consistent with the given road spectrum.

In order to verify the accuracy of reconstructed pavement, the power spectrum density of pavement roughness is analyzed by Welch's method, and the power spectral density of pavement roughness is compared with that of standard pavement.

As shown in Figure 3, the power spectral density of the pavement of grade "I" reconstructed and that of the standard pavement of grade "I" are shown. Due to lack of space, only the pavement of grade "I" is shown in this paper, and "B"~"H" pavements are not shown here. Figure 3 shows that the spatial frequency double logarithmic function of the power spectral density curve of standard pavement roughness is linear distribution. The power spectral density curve of simulated pavement elevation is obtained by using harmonic superposition method which is in high agreement with the power spectral density curve of standard pavement.

Table 2 shows that the root mean squares of pavement roughness of grade "A"~"H" reconstructed are within the standard range and very close to the standard value of road

TABLE 2: Classification of pavement roughness.

Grade	$G_q(n_0)/10^{-6}m^3$ ($n_0 = 0.1 m^{-1}$)			$\sigma_q/10^{-3} m \cdot 0.011 m^{-1} < n < 2.83 m^{-1}$			$\sigma_q/10^{-3} m$	
	Lower limit	Geometric mean value of road roughness coefficient	Upper limit	Lower limit	Root mean square of road roughness	Upper limit	Root mean square of reconstructed road roughness	
“I”	8	16	32	2.69	3.81	5.38	3.7	
“II”	32	64	128	5.38	7.61	10.77	7.7	
“III”	128	256	512	10.77	15.23	21.53	14.7	
“IV”	512	1024	2048	21.53	30.45	43.06	30.2	
“V”	2048	4096	8192	43.06	60.9	86.13	61	
“VI”	8192	16384	32768	86.13	121.8	172.26	121.2	
“VII”	32768	65536	131072	172.26	243.61	344.52	238	
“VIII”	131072	262144	524288	344.52	487.22	689.04	491.1	

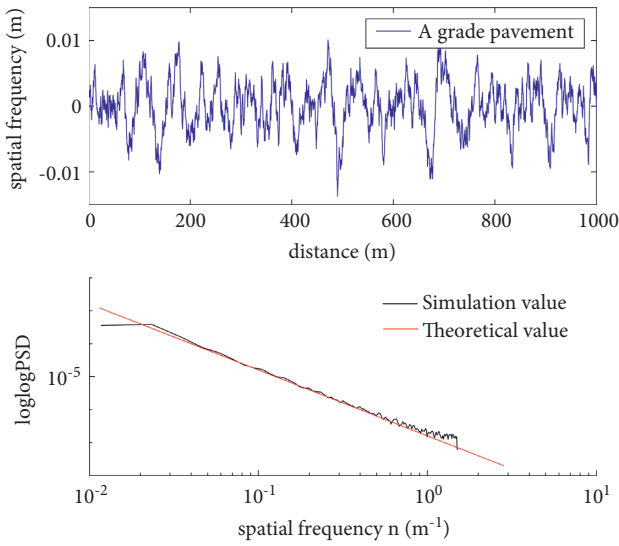


FIGURE 3: Grade “I” pavement roughness.

roughness. The pavement roughness reconstructed by harmonic superposition method is in line with the standard.

The reconstructed pavement roughness is incorporated into road geometry to develop three-dimensional road surface models. The road models are imported into CarSim, and the coupling model of human-vehicle-road-road environment is developed in CarSim. The lateral acceleration and lateral force coefficient are used to characterize vehicle’s rollover and skidding, respectively. The effects of road factors considering pavement roughness on vehicle rollover and skidding are then studied.

6. Design of Experiment of Vehicle Dynamics Simulation

In order to study the influence of various road factors on vehicle driving safety through relatively few and highly representative simulations, the orthogonal test method is used. This paper analyzes the influence of horizontal curve (A), grade (B), superelevation (C), road adhesion coefficient (D), vehicle speed (E), and pavement roughness (F) on vehicle rollover and skidding, and the horizontal curve interacts with grade ($A \times B$), horizontal curve interacts with superelevation ($A \times C$), and horizontal curve interacts with

road adhesion coefficient ($A \times D$) which are also considered. The level of each factor is shown in Table 3, each of which contains three factor levels.

The road studied in this paper is highway, road width is 3.75 m, and there are transition sections. The design speed levels are 80 km/h, 100 km/h, and 120 km/h. The levels of all road factors are selected based on these different design speeds. According to the design specification for highway alignment [75], the minimum radius of horizontal curve with design speed of 120 km/h is 650 m. Therefore, the radius of horizontal curve is greater than this value. The road radius selected in this study is shown in Table 3. For the grade level, horizontal, upslope, and downslope sections are selected. The grade is designed between the maximum and the minimum value. The superelevation selection is evenly distributed within the range allowed by the specification.

Snow covered pavement (0.2), wet pavement (0.5), and dry pavement (0.8) are studied. Highway pavement spectrum in China is generally within the range of “I,” “II,” and “III” [76]. Pavement roughness of almost of all newly-built highways is grade “I.” Most of the pavements with longer operation time are in grade “II” and some of them are in grade “III” or “IV” [77]. Rough road surface of the ISO “IV” grade is not usual in the paved road but refers to an unpaved road surface extremely irregular. In this paper, road surface roughness of grade “I,” “II,” and “IV” is studied. Orthogonal table of $L_{27}(3^{13})$ is selected. The parameters of 27 road models are imported by CarSim. According to the literature [78], the position of each interaction factor can be obtained, and the blank column is used as the error term. Table 4 shows the orthogonal table of 27 road models and the safety margin of rollover and skidding obtained by vehicle dynamics simulation.

7. Effect of Pavement Roughness on Vehicle Rollover and Skidding

7.1. Vehicle Rollover. Table 5 is the variance analysis of safety margin of vehicle rollover. Some factors have no significant effect on the results. That is, the sum of squares of this factor is much less than that of error terms. Specifically, we see $\overline{S_B} < \overline{S_e}$, $\overline{S_C} < \overline{S_e}$, $\overline{S_D} < \overline{S_e}$, $\overline{S_{A \times B}} < \overline{S_e}$, $\overline{S_{A \times C}} < \overline{S_e}$, and $\overline{S_{A \times D}} < \overline{S_e}$. Therefore, the sum of squares of factors with marginal effect is absorbed into a single new error term e . The square error and the new degree of freedom are obtained as follows: $S_e =$

TABLE 3: Factors and levels considered in simulation of vehicle dynamics.

Level	A Radius of horizontal curve (m)	B Grade (%)	C Superelevation (%)	D Road adhesion coefficient	E Vehicle speed (km/h)	F Grades of road surface roughness
1	700	-4	4	0.2	80	"I"
2	1000	0	6	0.5	100	"II"
3	1500	4	8	0.8	120	"IV"

TABLE 4: Orthogonal design and simulation results.

Factors Column	A 1	B 2	A × B ₁ 3	A × B ₂ 4	C 5	A × C ₁ 6	A × C ₂ 7	D 8	A × D ₁ 9	A × D ₂ 10	E 11	F 12	13	M ₁ (g)	M ₂
1	1	1	1	1	1	1	1	1	1	1	1	1	1	0.5545	0.0532
2	1	1	1	1	2	2	2	2	2	2	2	2	2	0.5166	0.3097
3	1	1	1	1	3	3	3	3	3	3	3	3	3	0.4684	0.622
4	1	2	2	2	1	1	1	2	2	2	3	3	3	0.4668	0.238
5	1	2	2	2	2	2	2	3	3	3	1	1	1	0.5582	0.6865
6	1	2	2	2	3	3	3	1	1	1	2	2	2	0.5178	0.0574
7	1	3	3	3	1	1	1	3	3	3	2	2	2	0.5174	0.6317
8	1	3	3	3	2	2	2	1	1	1	3	3	3	0.4664	0.0176
9	1	3	3	3	3	3	3	2	2	2	1	1	1	0.5582	0.3464
10	2	1	2	3	1	2	3	1	2	3	1	2	3	0.5772	0.068
11	2	1	2	3	2	3	1	2	3	1	2	3	1	0.5501	0.3467
12	2	1	2	3	3	1	2	3	1	2	3	1	2	0.5158	0.6726
13	2	2	3	1	1	2	3	2	3	1	3	1	2	0.5151	0.2898
14	2	2	3	1	2	3	1	3	1	2	1	2	3	0.5789	0.6868
15	2	2	3	1	3	1	2	1	2	3	2	3	1	0.5508	0.074
16	2	3	1	2	1	2	3	3	1	2	2	3	1	0.5505	0.668
17	2	3	1	2	2	3	1	1	2	3	3	1	2	0.5153	0.0434
18	2	3	1	2	3	1	2	2	3	1	1	2	3	0.5789	0.3467
19	3	1	3	2	1	3	2	1	3	2	1	3	2	0.5953	0.0683
20	3	1	3	2	2	1	3	2	1	3	2	1	3	0.5761	0.3545
21	3	1	3	2	3	2	1	3	2	1	3	2	1	0.553	0.6857
22	3	2	1	3	1	3	2	2	1	3	3	2	1	0.5532	0.331
23	3	2	1	3	2	1	3	3	2	1	1	3	2	0.5952	0.687
24	3	2	1	3	3	2	1	1	3	2	2	1	3	0.5764	0.0787
25	3	3	2	1	1	3	2	3	2	1	2	1	3	0.5763	0.6903
26	3	3	2	1	2	1	3	1	3	2	3	2	1	0.5535	0.0678
27	3	3	2	1	3	2	1	2	1	3	1	3	2	0.5952	0.3469

TABLE 5: Variance analysis of safety margin of vehicle's rollover.

Source of variance	Absorbed into e	Sum of squares, S	Freedom, f	Mean square, \bar{S}	F value	Significance	Critical value
A	No	0.017	2	0.0085	184.38	Highly	
B	Yes	1.916E-6	2	9.58E-7			
C	Yes	3.736E-6	2	1.868E-6			
D	Yes	2.352E-6	2	1.176E-6			
E	No	0.019	2	0.0095	206.52	Highly	$F_{1-0.1}(2, 22) = 2.56F_{1-0.05}(2, 22) = 3.44F_{1-0.01}(2, 22) = 5.72F_{1-0.1}(4, 22) = 2.22F_{1-0.05}(4, 22) = 2.82F_{1-0.01}(4, 22) = 4.31$
F	No	0.001	2	0.0005	10.87	Highly	
(A × B)	Yes	7.282E-7	4	1.8205E-7			
(A × C)	Yes	2.935E-6	4	7.3375E-7			
(A × B)	Yes	3.06E-6	4	7.65E-7			
e	No	0.001	2	0.0005			
e^Δ	—	1.0147E-3	22	4.61E-5			

$$S_e + S_B + S_C + S_D + S_{A \times B} + S_{A \times C} + S_{A \times D} + S_e = 1.012 \times 10^{-3}$$

and $f_e = f_e + f_B + f_C + f_D + f_{A \times B} + f_{A \times C} + f_{A \times D} + f_e = 22$.

The variance test is performed through the formula $F = S_j / f_j / S_{e\Delta} / f_{e\Delta}$. If $F \geq F_{1-\alpha}(f_j, f_{e\Delta})$, the significance of the influence of this factor on the results was inferred by significance α . If $F_j \geq F_{1-0.01}(f_j, f_e)$, this factor has a highly significant effect on the results. If $F_{1-0.01}(f_j, f_e) > F_j \geq F_{1-0.05}(f_j, f_e)$, this factor has a significant effect on the results. If $F_{1-0.05}(f_j, f_e) > F_j \geq F_{1-0.1}(f_j, f_e)$, the influence of this factor on the results is generally significant. If $F_{1-0.1}(f_j, f_e) > F_j$, this factor has no significant effect on the results.

Table 5 shows F values of horizontal curve (A), vehicle speed (E), and road surface roughness (F) are greater than $F_{1-0.01}(2, 22) = 5.72$, so the influence of horizontal curve, vehicle speed, and road surface roughness on safety margin of vehicle rollover is highly significant. "Highly significance" indicates that the factor has a highly significant effect on the test results. The influence of grade (B) and superelevation (C) and road adhesion coefficient (D) on the safety margin of vehicle rollover is not significant.

Figure 4 shows the influence of horizontal curve on vehicle rollover. The vehicle speed is 80 km/h, and the road adhesion coefficient is 0.8 (good pavement). The pavement roughness is grade "II." The grade is zero, and road camber is designed as 2%. The radius of horizontal curve is 500 m, 600 m, 700 m, 800 m, and 900 m, respectively. In the studied road section, the vehicle starts from the straight section and passes through the curve steadily. The traveling time between 9 s and 45 s was studied.

The first section is a straight section, the middle is a transition curve section, and the last is a circular curve section. Figure 4 shows safety margin of vehicle rollover is not affected in the straight section. In the transition curve section, with the increase of the radius of the horizontal curve, the safety margin of the vehicle rollover decreases. In the circular curve section, the safety margin of the vehicle rollover is steady at the minimum value, and with the increase of circle curve radius, the stability value of rollover safety margin is smaller. That is to say, the vehicle is more prone to rollover with the decrease of horizontal curve radius.

Figure 5 shows the influence of vehicle speed on safety margin of vehicle's rollover. The radius of horizontal curve is 1000 m, and the road adhesion coefficient is 0.8. The pavement roughness is grade "II." The grade is not designed, and road camber is 2%. The vehicle speed is 80 km/h, 90 km/h, 100 km/h, 110 km/h, and 120 km/h, respectively. Figure 6 shows that the greater the vehicle speed, the smaller the safety margin of vehicle rollover, and the vehicle is more prone to rollover.

Figure 6 shows the influence of pavement roughness on safety margin of vehicle rollover when the road is a curve. The vehicle speed is 80 km/h. The radius of horizontal curve is 1000 m, and the road adhesion coefficient is 0.8, no grade, and road camber is designed as 2%. The pavement roughness of grade "I," "II," "III," and "IV" is studied, respectively. According to Figure 6, with the change of pavement

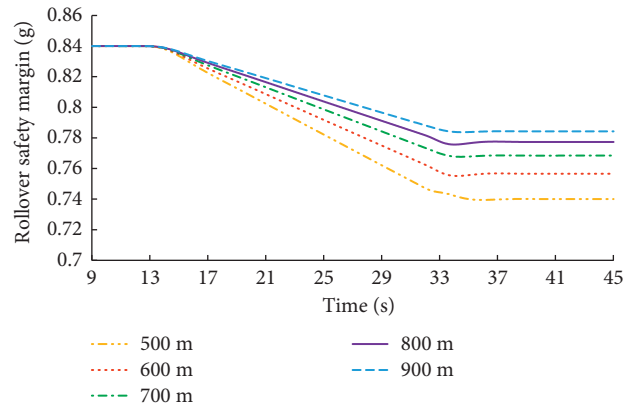


FIGURE 4: Influence of horizontal curve on safety margin of vehicle rollover.

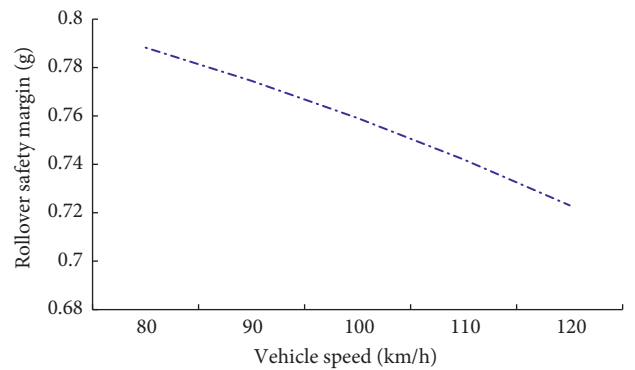


FIGURE 5: Influence of vehicle speed on safety margin of vehicle rollover.

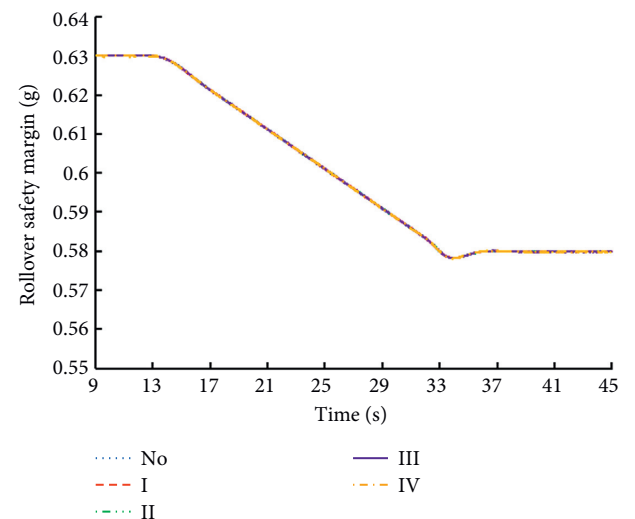


FIGURE 6: Effect of pavement roughness on safety margin of vehicle rollover (curve).

roughness level, the safety margins of vehicle rollover are coincident. Namely, with the change of pavement roughness level, the change of safety margin of vehicle rollover is not obvious. According to Table 5, F value of horizontal curve is

far greater than that of road roughness. It means that when there are both curves and road roughness, the influence of pavement roughness is negligible as compared to that of the curve.

In order to further study the influence of pavement roughness on safety margin of vehicle rollover. The straight road sections are studied, as shown in Figure 7. Figure 7 shows that the pavement roughness of grade “I” and “II” has little influence on safety margin of vehicle rollover. These values are steady at the maximum rollover safety margin (0.84 g). It also shows that the fluctuation range of the curve of the safety margins of vehicle rollover corresponding to roughness grade “II” is greater than that of roughness grade “I.” Figure 7 shows that the safety margins of vehicle rollover of grade “III” and “IV” are smaller than that of “I” and “II.” The curves of grade “III” and “IV” coincide. These values are steadily at 0.83 g. The fluctuation range of the curve of grade “IV” is larger than that of grade “III.” The analysis indicates that the greater the pavement roughness grade is, the smaller the safety margin of vehicle rollover is. In other words, the vehicle is more prone to rollover.

7.2. Vehicle Skidding. Table 6 shows variance analysis of safety margin of vehicle skidding. The F values of horizontal curve (A), road adhesion coefficient (D), and vehicle speed (E) in Table 6 are greater than $F_{1-0.01}(2, 16) = 6.23$, so the impact of these factors is highly significant on safety margin of vehicle skidding. The F value of superelevation (C) is greater than $F_{1-0.05}(2, 16) = 3.63$ and less than $F_{1-0.01}(2, 16) = 6.23$, so the superelevation has a significant impact on the safety margin of vehicle skidding. “Highly significance” indicates that the factor has a highly significant effect on the test results. The impact of grade (B) and pavement roughness (F) on the safety margin of vehicle skidding is not significant.

Figure 8(a) shows the influence of horizontal curve on safety margin of vehicle skidding; the design parameters in Figure 5(a) are consistent with that of Figure 5. Figure 8(a) shows that the larger the radius of horizontal curve is, the greater the safety margin of vehicle skidding is, and the vehicle is more prone to skidding. Figure 8(b) is the influence of vehicle speed on the safety margin of vehicle skidding; the design parameters in Figure 8(b) are consistent with that of Figure 6. Figure 8(b) shows that the higher the vehicle speed is, the smaller the safety margin of vehicle skidding is, and the vehicle is more prone to skidding.

Figure 8(c) is the influence of the superelevation on the safety margin of vehicle skidding. The vehicle speed is 80 km/h, the road adhesion coefficient is 0.8, no grade and road roughness, the radius of horizontal curve is 300m, and the superelevation is 0.02, 0.04, 0.06, 0.08, and 0.1, respectively. Figure 8(c) shows that the larger the superelevation is, the greater the safety margin of vehicle skidding is, and the vehicle is not prone to skidding.

Figure 8(d) is the influence of road adhesion coefficient on the safety margin of vehicle skidding. The vehicle speed is 80 km/h; the road adhesion coefficient is 0.8. The pavement roughness is grade “II.” The grade is not designed. The radius

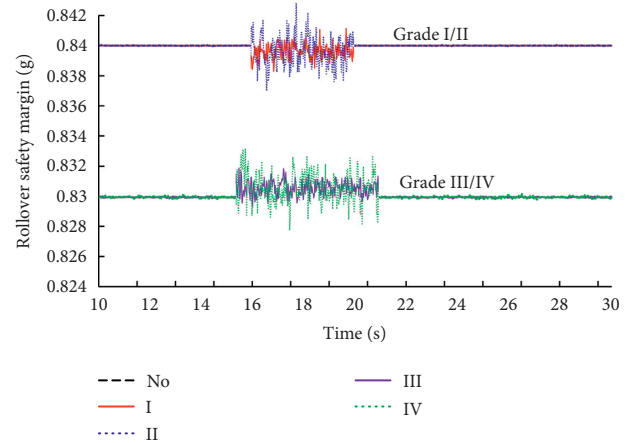


FIGURE 7: Effect of pavement roughness on safety margin of vehicle rollover (straight line).

of horizontal curve is 1000 m, and the superelevation is set as 0.2, 0.3, 0.5, 0.7, and 0.8. Figure 8(d) shows that the greater the road adhesion coefficient is, the greater the safety margin of vehicle skidding is, and the vehicle is not prone to skidding.

8. Pavement Differential Settlement

8.1. Pavement Differential Settlement due to Bridge Widening. Fanyang River Bridge is widened on the left and right sides to accommodate more lanes for traffic. The old bridge is 366.04 m long and 28 m wide. The geometric alignment of the new bridge is consistent with those of the old bridge. Cross view of the widened Fanyang River Bridge is shown in Figure 9, in which two new bridges with a width of 6.5 m are added to the left and right sides of the old bridge. Each new bridge consists of two lanes, with each lane having a width of 3.75 m (CCCC First Highway Consultants Co., 2017). After the completion of the new bridge, five lanes are on the right side and five lanes are on the left side.

The scenario considered in this study is that there is a differential settlement in pavement at the joint between the old and new bridges, as shown in Figure 10. Assume that the left side of the joint is the old bridge lane and the right side is the new bridge lane in the direction of the vehicle. A 140 m long bridge section is studied, which is a straight segment with no grade and no superelevation. When a vehicle crossing the joint to make a lane change from the old bridge (the red part in Figure 10) to the bridge (the blue part in Figure 10), the trajectory of the vehicle traverses the differential settlement, as shown in Figure 11, posing some risks to vehicle stability.

This section studies the influence of settlement differences of widened bridges on the risk of vehicle rollover and skidding under different pavement conditions. Lateral acceleration and lateral force coefficient are used to characterize vehicle’s rollover and skidding, respectively. A human-vehicle-bridge coupling dynamic model is developed in CarSim. In the simulation model, a number of assumptions are made, including that there is a 45° slope at the joint of the

TABLE 6: Analysis of vehicle skidding safety margin variance.

Source of variance	Sum of squares, S	Freedom, f	Mean square, \bar{S}	F value	Significance	Critical value
A	0.007	2	0.0035	12.93	Highly	
B	0	2	0			
C	0.002	2	0.001	3.70	Significance	
D	1.369	2	0.684	2527.72	Highly	
E	0.006	2	0.003	11.09	Highly	
F	0.001	2	0.0005			
$(A \times B)$	$1.618E-04$	4	$4.05E-05$			
$(A \times C)$	$6.633E-04$	4	$1.65825E-04$			
$(A \times D)$	$2.504E-04$	4	$6.26E-05$			
e	0.002	2	0.001			
e^Δ	$4.330E-03$	16	$2.706E-04$			

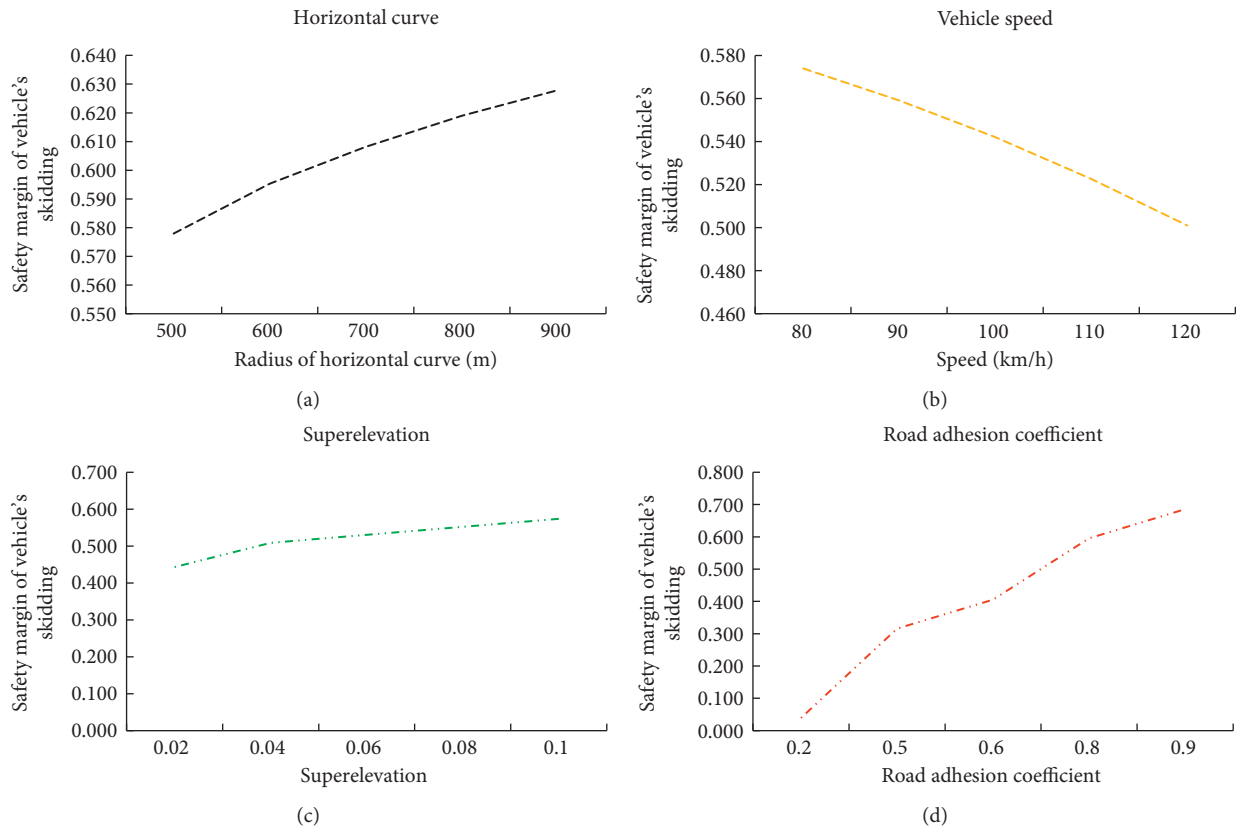


FIGURE 8: Influence of single factor on safety margin of vehicle's skidding. (a) Horizontal curve. (b) Vehicle speed. (c) Superelevation. (d) Road adhesion coefficient.

new and old bridges, as shown in the yellow circle in Figure 11; the vehicle is traveling at a steady speed of 50 km/h when changing lanes. To study the influence of pavement condition and settlement difference on road safety, three levels of road adhesion coefficient are considered: 0.8 (dry pavement), 0.5 (wet asphalt pavement), and 0.2 (compacted snow pavement), and five levels of settlement difference are considered: 1 cm, 2 cm, 3 cm, 4 cm, and 5 cm, respectively.

8.2. *Effect of Pavement Differential Settlement on Vehicle Rollover and Skidding.* Figure 12 shows the influence of settlement difference on the safety margin of vehicle

skidding, when the road adhesion coefficients of the bridge are 0.2, 0.5, and 0.8, respectively. Figure 12 shows that when the road adhesion coefficient is small (0.2, 0.5), the safety margin of vehicle skidding is less affected by settlement difference. When the road adhesion coefficient of the bridge is 0.2, the safety margin of vehicle skidding is less than 0, which indicates that the vehicle has skidded. The vehicle will deviate from the original driving lane and collide with the vehicle in the adjacent lane. If obstacles or potholes are encountered in the process of skidding, the vehicle is likely to roll over. This phenomenon is related to the low road adhesion coefficient.

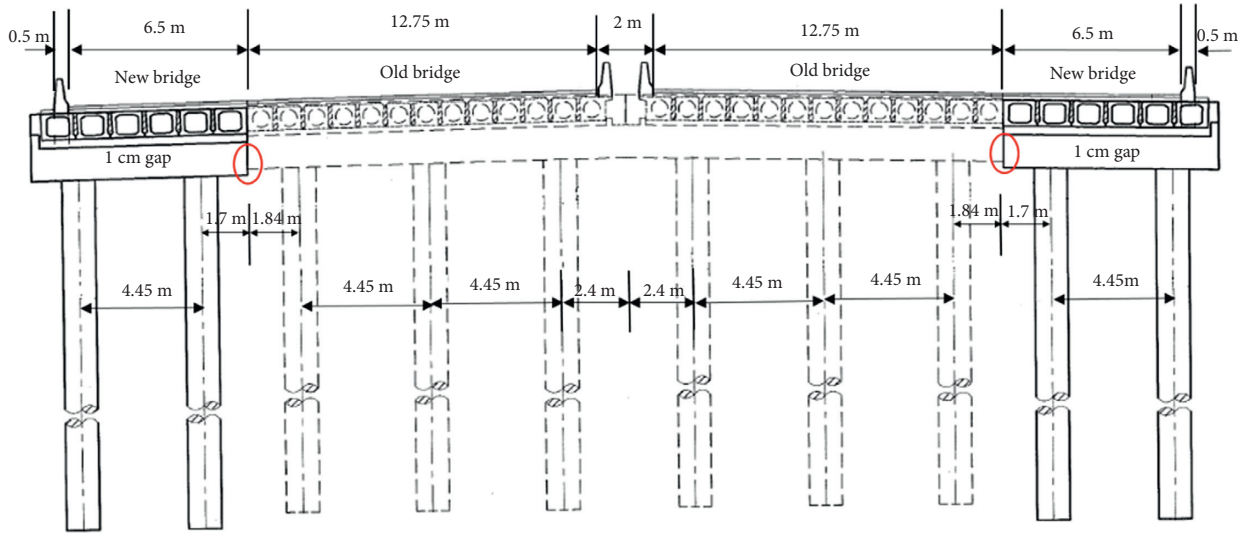


FIGURE 9: Cross view of the widened Fanyanghe Bridge.

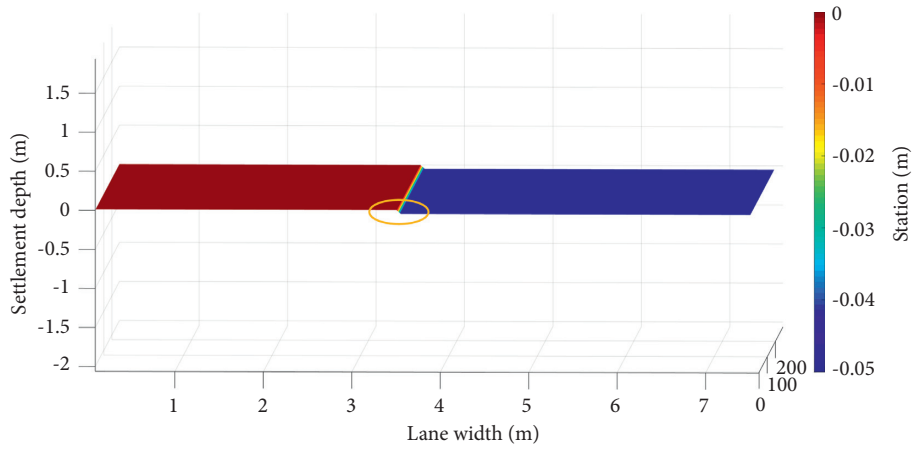


FIGURE 10: Three-dimensional model of the bridge.

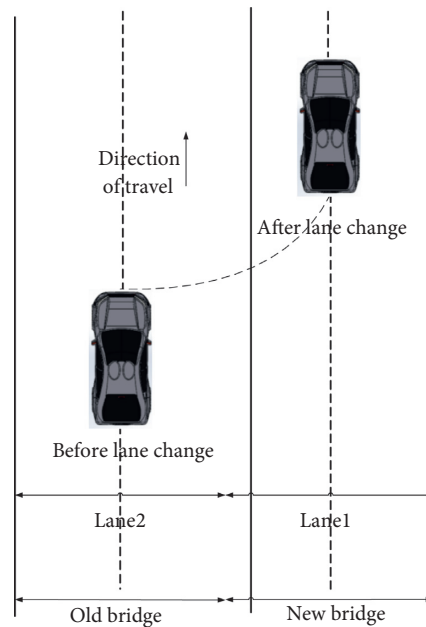


FIGURE 11: Lane-changing trajectory of the vehicle.

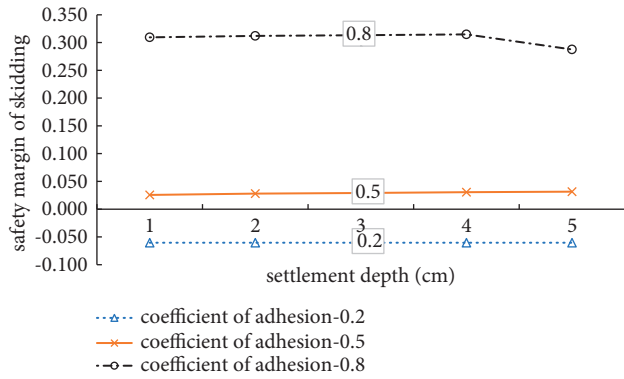


FIGURE 12: The influence of pavement settlement difference on vehicle skidding.

When the road adhesion coefficient is 0.5, the safety margin of vehicle skidding is less than 0.1. Although the vehicle will not skid, the vehicle is prone to skidding due to the low safety margin. When the road adhesion coefficient is 0.8, the safety margin of vehicle skidding is high, and the possibility of vehicle skidding is low. However, when settlement difference is 1–4 cm, the safety margin of vehicle skidding is not affected. When the settlement difference is 5 cm, the safety margin of vehicle skidding decreases. It is thus clear that when the settlement difference is 5 cm, the driving safety of vehicles will be affected.

Figure 13 shows the influence of settlement difference of new and old bridges on vehicle rollover, when the road adhesion coefficients of the bridge are 0.2, 0.5 and 0.8, respectively. Figure 13 shows that when the road adhesion coefficients are 0.5 and 0.8, the safety margin of vehicle rollover is little affected by the settlement difference, and the two curves basically coincide. When the adhesion coefficient is 0.2, the safety margin of vehicle rollover decreases with the increase of settlement difference. The analysis indicates that when the road adhesion coefficient is low, the vehicle rollover is greatly affected by the settlement difference.

In addition, Figure 13 shows that when the road adhesion coefficient is 0.2, the safety margin of vehicle rollover is greater than that when the road adhesion coefficients are 0.5 and 0.8, respectively. That is, when the road adhesion coefficient is 0.2, the vehicle is not more prone to rollover. Based on the above analysis of skidding, when the road adhesion coefficient is 0.2, the vehicle has skidded when changing lanes. It is thus clear that vehicle skidding has an impact on vehicle rollover, and vehicle skidding will reduce the possibility of vehicle rollover (nontripped rollover).

8.3. Effect of Vehicle Speed on Rollover and Skidding when Crossing Differential Settlement. To study the influence of vehicle speed on driving safety of vehicle when there is settlement difference, the settlement difference is designed at 5 cm. The road adhesion coefficient is designed at 0.8. The vehicle changes lanes at speeds of 50 km/h, 60 km/h, 70 km/h, 80 km/h, and 90 km/h, respectively; the safety margin of vehicle rollover and skidding is shown in Figure 14. Figure 14

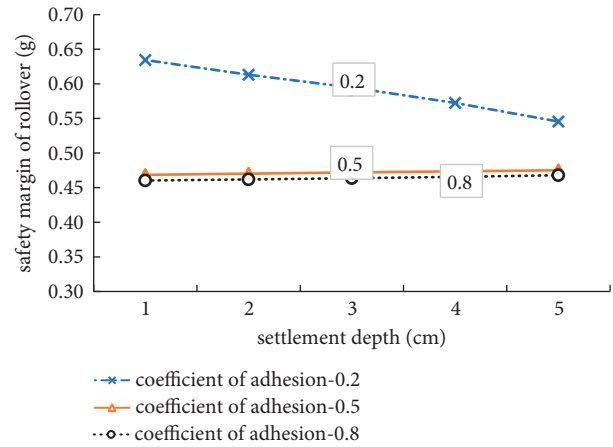


FIGURE 13: The influence of pavement settlement difference on vehicle rollover.

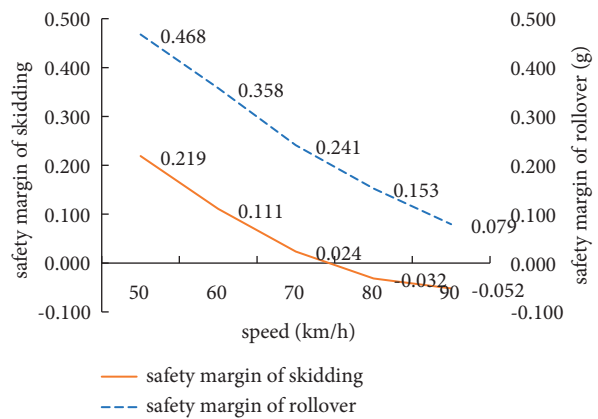


FIGURE 14: Influence of vehicle speed on vehicle skidding and rollover.

shows that the safety margin of vehicle rollover and skidding decreases with the increase of vehicle speed. When the speed is 70 km/h, the safety margin of vehicle skidding is 0.024, which is very low and the vehicle is prone to skidding. When the vehicle speeds are 80 km/h and 90 km/h, the safety margin of vehicle skidding is less than 0, and theoretically, the vehicle has skidded.

When the vehicle speed is less than 80 km/h, the safety margin of vehicle rollover is greater than 0.1, and the vehicle is not prone to rollover. When the speed is 90 km/h, the safety margin of vehicle rollover is 0.079, which is very low and the vehicle is prone to rollover.

Figure 14 shows that when the settlement difference between the new and old bridges is 5 cm, the lane-changing speed of vehicles has a great influence on the safety margin of vehicle rollover and skidding. When the lane-changing speed is greater than or equal to 70 km/h, the vehicle is prone to skidding. When the lane-changing speed is greater than or equal to 90 km/h, the vehicle is prone to rollover. Therefore, when the settlement difference is greater than or equal to 5 cm, the vehicle speed should be strictly controlled. In addition, because the scale of primary ordinate and secondary ordinate is consistent,

the safety margin of vehicle rollover and skidding can be compared. Figure 14 shows that the safety margin of rollover is always greater than that of skidding. Namely, when the settlement difference is 5 cm and the road adhesion coefficient is 0.8, it is more prone to skidding than rollover.

9. Concluding Remarks

The influence of pavement roughness on vehicle rollover is significant, while the influence of pavement roughness on vehicle skidding is not significant. The higher the grade of pavement roughness, the smaller the safety margin of vehicles rollover. The influence of pavement roughness of grade A and B on vehicle rollover is negligible. Pavement roughness of grade C and D significantly reduces safety margin of vehicle rollover. As pavement roughness further deteriorates to grades lower than D, the safety margin of vehicle rollover gets further reduced. Therefore, pavement roughness should be considered in road safety study. Timely pavement maintenance to restore evenness of pavement surface is critical to improve road safety.

When road adhesion coefficients of the bridge are 0.2 and 0.5, and vehicles change lanes at a speed of 50 km/h, the safety margin of vehicle skidding is not affected by the settlement difference. When the road adhesion coefficient of the bridge is 0.8 and the settlement difference is between 1 cm and 4 cm, the safety margin of vehicle skidding is not affected by the settlement difference. When the settlement difference is 5 cm, the safety margin of vehicle skidding reduces. The settlement difference of 5 cm can be used as a reasonable standard for pavement maintenance from road safety point of view. When the road adhesion coefficients of the bridge are 0.5 and 0.8, and vehicles change lanes at a speed of 50 km/h, the safety margin of vehicle rollover is little affected by the settlement difference. When the road adhesion coefficient is 0.2, the safety margin of vehicle rollover decreases with the increase of settlement difference.

It is also found that vehicle skidding can reduce the risk of nontripped rollover. When the settlement difference is 5 cm and the road adhesion coefficient is 0.8, the safety margin of vehicle skidding and rollover decreases with the increase of lane-changing speed of vehicles, and the vehicle is more prone to skidding than rollover. When the settlement difference is greater than or equal to 5 cm, vehicle lane-changing speed should not exceed 70 km/h. For the sake of traffic safety, lane-changing speed of vehicles should be strictly controlled.

Data Availability

All data, models, and codes generated or used during the study appear in the submitted article.

Conflicts of Interest

The authors declare that they have no conflicts of interest.

Acknowledgments

This study was sponsored by Shangdong Expressway Co., Ltd., under grant 2017-BLK4, and in part by the National Science Foundation under Grant CMMI-0644552, and the National Science Foundation of China under Grant U1134206, to which the authors are grateful.

References

- [1] NHTSA, *Traffic Safety Facts: 2016: A Compilation of Motor Vehicle Crash Data from the Fatality Analysis Reporting System and the General Estimates System*, NHTSA, U.S. Department of Transportation, Washington, DC, 2016, <https://www.nhtsa.dot.gov>.
- [2] S. Dadvar, Y. J. Lee, and H. S. Shin, "Improving crash predictability of the Highway Safety Manual through optimizing local calibration process," *Accident Analysis & Prevention*, vol. 136, Article ID 105393, 2020.
- [3] A. Kassua and M. Anderson, "Analysis of severe and non-severe traffic crashes on wet and dry highways," *Transportation Research Interdisciplinary Perspectives*, vol. 2, Article ID 100043, 2019.
- [4] T. U. Saeed, T. Hall, T. Baroud, and M. J. Volovski, "Analyzing road crash frequencies with uncorrelated and correlated random-parameters count models: an empirical assessment of multilane highways," *Analytic Methods in Accident Research*, vol. 23, Article ID 100101, 2019.
- [5] M. Borsati, M. Cascarano, and F. Bazzana, "On the impact of average speed enforcement systems in reducing highway accidents: evidence from the Italian Safety Tutor," *Economics of Transportation*, vol. 20, Article ID 100123, 2019.
- [6] P. Q. Li and J. He, "Geometric design safety estimation based on tire-road side friction," *Transportation Research Part C*, vol. 63, pp. 114–125, 2016.
- [7] A. Morgan and F. L. Mannering, "The effects of road-surface conditions, age, and gender on driver-injury severities," *Accident Analysis & Prevention*, vol. 43, pp. 1852–1863, 2011.
- [8] T. Kim, D. Bose, and J. Foster, "Identification of characteristics and frequent scenarios of single-vehicle rollover crashes during pre-ballistic phase; part 1 – a descriptive study," *Accident Analysis & Prevention*, vol. 107, pp. 31–39, 2017.
- [9] D. C. Viano and C. Parenteau, *Case Study of Vehicle Maneuvers Leading to Rollovers: Need for a Vehicle Test Simulating Off-Road Excursions, Recovery and Handling*, SAE International, PA, USA, 2003.
- [10] L. Sun and K. S. You, "Reliability-based risk analysis of vehicle moving on curved sections considering multiple failure modes," *China Journal of Highway and Transport*, vol. 26, no. 4, pp. 36–42, 2013.
- [11] K. S. You and L. Sun, "Reliability analysis of vehicle stability on combined horizontal and vertical alignments: driving safety perspective," *Journal of Transportation Engineering*, vol. 139, pp. 804–813, 2013.
- [12] Y. Yin, H. Wen, L. Sun, and W. Hou, "Study on the influence of road geometry on vehicle lateral instability," *Journal of Advanced Transportation*, vol. 2020, Article ID 7943739, 15 pages, 2020.
- [13] Y. Yin, H. Wen, L. Sun, and W. Hou, "The influence of road geometry on vehicle rollover and skidding," *International Journal of Environmental Research and Public Health*, vol. 17, 2020.

- [14] H. Y. Wen, J. B. Wu, and W. W. Qi, "CP-CS fusion model for on-ramp merging area on the highway," *Journal of South China University of Technology*, vol. 48, no. 2, pp. 50–57, 2020.
- [15] L. Sun and X. Deng, "Predicting vertical dynamic loads caused by vehicle-pavement interaction," *Journal of Transportation Engineering*, ASCE, vol. 126, no. 5, pp. 470–478, 1998.
- [16] L. Sun and B. S. Greenberg, "Dynamic response of linear systems to moving stochastic sources," *Journal of Sound and Vibration*, vol. 229, no. 4, pp. 957–972, 2000.
- [17] L. Sun, "Developing spectrum-based models for international roughness index and present serviceability index," *Journal of Transportation Engineering*, ASCE, vol. 127, no. 6, pp. 463–470, 2001.
- [18] L. Sun, "On human perception and evaluation to road surfaces," *Journal of Sound and Vibration*, vol. 247, no. 3, pp. 547–560, 2001.
- [19] L. Sun, "Computer simulation and field measurement of dynamic pavement loading," *Mathematics and Computers in Simulation*, vol. 56, no. 3, pp. 297–313, 2001.
- [20] L. Sun, "Optimum design of road-friendly vehicle suspension systems subject to rough road surface," *Applied Mathematical Modelling*, vol. 26, no. 5, pp. 635–652, 2002.
- [21] L. Sun, "Simulation of pavement roughness and IRI based on power spectral density," *Mathematics and Computers in Simulation*, vol. 61, pp. 77–88, 2003.
- [22] L. Sun, "Analytical dynamic displacement response of rigid pavements to moving concentrated and line loads," *International Journal of Solids and Structures*, vol. 43, pp. 4370–4383, 2006.
- [23] L. Sun, "An overview of a unified theory of dynamics of vehicle-pavement interaction under moving and stochastic load," *Journal of Modern Transportation*, vol. 21, no. 3, pp. 135–162, 2013.
- [24] L. Sun and J. Su, "Modeling random fields of road surface irregularities," *International Journal of Road Materials and Pavement Design*, vol. 2, no. 1, pp. 49–70, 2001.
- [25] L. Sun and T. W. Kennedy, "Spectral analysis and parametric study of stochastic pavement loads," *Journal of Engineering Mechanics*, ASCE, vol. 128, no. 3, pp. 318–327, 2002.
- [26] L. Sun, Z. Zhang, and J. Ruth, "Modeling indirect statistics of surface roughness," *Journal of Transportation Engineering*, ASCE, vol. 127, no. 2, pp. 105–111, 2001.
- [27] L. Sun, X. Cai, and J. Yang, "Genetic algorithm-based optimum vehicle suspension design using minimum dynamic pavement load as a design criterion," *Journal of Sound and Vibration*, vol. 301, no. 1-2, pp. 18–27, 2006.
- [28] L. Sun, W. Kenis, and W. Wang, "Stochastic spatial excitation induced by a distributed contact with homogenous Gaussian random fields," *Journal of Engineering Mechanics*, ASCE, vol. 132, no. 7, pp. 714–722, 2006.
- [29] L. Sun and K. You, Y. Wang, D. Wang, and W. Gu, Influence analysis of road conditions on vehicle rollover," *Journal of Southeast University*, vol. 43, no. 3, pp. 644–648, 2013.
- [30] K. You, L. Sun, and W. Gu, "Reliability design theory and method of highway horizontal curve radii," *Journal of Traffic and Transportation Engineering*, vol. 12, no. 6, pp. 1–6, 2012.
- [31] K. You, L. Sun, and W. Gu, "Risk analysis-based identification of road hazard locations using vehicle dynamic simulation," *Journal of Southeast University*, vol. 42, no. 1, pp. 150–155, 2012.
- [32] K. You, L. Sun, and W. Gu, "Reliability-based risk analysis of roadway horizontal curve," *Journal of Transportation Engineering*, ASCE, vol. 138, no. 8, pp. 1071–1081, 2012.
- [33] L. Sun and K. You, "Reliability analysis of vehicle stability on combined horizontal and vertical alignments: a driving safety perspective," *Journal of Transportation Engineering*, ASCE, vol. 139, no. 8, pp. 804–813, 2013.
- [34] A. J. Anarkooli, M. Hosseinpour, and A. Kardar, "Investigation of factors affecting the injury severity of single-vehicle rollover crashes: a random-effects generalized ordered probit model," *Accident Analysis & Prevention*, vol. 106, pp. 399–410, 2017.
- [35] M. Keall and S. Newstead, "Induced exposure estimates of rollover risk for different types of passenger vehicles," *Traffic Injury Prevention*, vol. 10, no. 1, pp. 30–36, 2009.
- [36] G. Azimi, A. Rahimi, and H. Asgari, "Severity analysis for large truck rollover crashes using a random parameter ordered logit model," *Accident Analysis & Prevention*, vol. 135, pp. 1–7, 2020.
- [37] Q. Wu, G. H. Zhang, C. Chen, R. Tarefder, H. Wang, and H. Wei, "Heterogeneous impacts of gender-interpreted contributing factors on driver injury severities in single-vehicle rollover crashes," *Accident Analysis & Prevention*, vol. 94, pp. 28–34, 2016.
- [38] C. Chen, G. H. Zhang, Z. Qian, R. A. Tarefder, and T. Zong, "Investigating driver injury severity patterns in rollover crashes using support vector machine models," *Accident Analysis & Prevention*, vol. 90, pp. 128–139, 2016.
- [39] B. Fréchède, A. S. McIntosh, R. Grzebieta, and M. R. Bambach, "Characteristics of single vehicle rollover fatalities in three Australian states (2000–2007)," *Accident Analysis & Prevention*, vol. 43, pp. 804–812, 2011.
- [40] C. M. Farmer and A. K. Lund, "Rollover risk of cars and light trucks after accounting for driver and environmental factors," *Accident Analysis & Prevention*, vol. 34, pp. 163–173, 2002.
- [41] W. Hu and E. T. Donnell, "Severity models of cross-median and rollover crashes on rural divided highways in Pennsylvania," *Journal of Safety Research*, vol. 42, pp. 375–382, 2011.
- [42] D. F. Chu, Z. L. Li, J. M. Wang, C. Wu, and Z. Hu, "Rollover speed prediction on curves for heavy vehicles using mobile smartphone," *Measurement*, vol. 130, pp. 404–411, 2018.
- [43] A. Tarko, T. Hall, M. Romero, and C. J. L. Guillermo, "Evaluating the rollover propensity of trucks—a roundabout example," *Accident Analysis & Prevention*, vol. 91, pp. 127–134, 2016.
- [44] D. W. Harwood and J. M. Mason, "Horizontal curve design for passenger cars and trucks," *Transportation Research Record*, vol. 1445, pp. 2–33, 1994.
- [45] S. Lapapong and S. N. Brennan, "Terrain-aware rollover prediction for ground vehicles using the zero-moment point method," in *Proceedings of the 2010 American control conference*, pp. 1501–1507, IEEE Service Center, Baltimore, MD, USA, July 2010.
- [46] S. Mavromatis, A. Laiou, and G. Yannis, "Safety assessment of control design parameters through vehicle dynamics model," *Accident Analysis & Prevention*, vol. 125, pp. 330–335, 2019.
- [47] T. L. Wang, M. Shahawy, and D. Z. Huang, "Dynamic response OF highway trucks," *Due To Road Surface Roughness*, vol. 49, no. 6, pp. 1055–1067, 1993.
- [48] P. E. Uys, P. S. Els, and M. Thoreson, "Suspension settings for optimal ride comfort of off-road vehicles travelling on roads with different roughness and speeds," *Journal of Terramechanics*, vol. 44, no. 2, pp. 163–175, 2007.
- [49] K. R. Kashyzadeh, M. J. O. A. Ghorabi, and A. Arghavan, "Investigating the effect of road roughness on automotive component," *Engineering Failure Analysis*, vol. 41, pp. 96–107, 2014.

- [50] R. R. Ma, X. H. Chen, and J. Yang, "A simulation analysis of vehicle-pavement coupling vibration," *Journal of Transport Information and Safety*, vol. 33, no. 2, pp. 103–109, 2015.
- [51] J. L. Zhang, R. F. Chen, and K. Yao, "Analysis on influence of road pavement roughness on vehicle vibration," *Journal of Highway and Transportation Research and Development*, vol. 36, no. 11, pp. 129–133, 2019.
- [52] P. Hu, Q. Dong, and X. D. Pan, "Critical wind velocity of vehicle sideslip and rollover Considering influence of pavement roughness," *Journal of Highway and Transportation Research and Development*, vol. 32, no. 2, pp. 134–139, 2015.
- [53] J. S. Ye and W. Q. Wu, "Research on key technologies for bridge widening of Shanghai-Nanjing Expressway," in *Proceedings of the National Conference on Strengthening, Reconstruction and Evaluation of Existing Bridges*, pp. 403–409, Institute of Highway Science, Ministry of Communications, Southeast University, Nanjing, China, May 2008.
- [54] S. Hong and S. Park, "Effect of vehicle-induced vibrations on early-age concrete during bridge widening," *Construction and Building Materials*, vol. 77, no. 2015, pp. 179–186, 2015.
- [55] X. Wang, Y. Cao, P. Y. Jiang, L. Niu, and N. Lyu, "The safety effect of open-median management on one-side widened freeways: a driving simulation evaluation," *Journal of Safety Research*, vol. 73, pp. 57–67, 2020.
- [56] Chs(China News Service), "Several traffic accidents caused by road icing caused by dusting and watering in Changzhou," 2018, <http://www.chinanews.com/>.
- [57] Y. Yi, "Accident of Hangzhou Bay bridge," 2019, https://www.sohu.com/a/275284537_467457.
- [58] K. N. Kan, "Accident of beihuan overpass in shenzhen," 2019, https://www.sohu.com/a/339081952_741362.
- [59] P. P. Fan, *Research on Safety Analysis and Security Technology of Highway Curved Bridge Based on Cross Section*, Jilin University, Changchun, China, 2017.
- [60] F. Chen, H. R. Peng, X. X. Ma, J. Liang, W. Hao, and X. Pan, "Examining the safety of trucks under crosswind at bridge-tunnel section: a driving simulator study," *Tunnelling and Underground Space Technology*, vol. 92, Article ID 103034, 2019.
- [61] Y. F. Zhou and S. R. Chen, "Fully coupled driving safety analysis of moving traffic on long-span bridges subjected to crosswind," *Journal of Wind Engineering and Industrial Aerodynamics*, vol. 143, pp. 1–18, 2015.
- [62] X. D. Pan, J. Y. Liang, and F. Chen, "Experimental method for driving simulation on the long-span," *Bridge Under Wind-vehicle-Bridge Coupling*, vol. 47, no. 6, pp. 787–794, 2019.
- [63] Q. L. Yu, X. J. Chen, and S. B. Jiang, "Analysis of safety wind velocity of driving on sea-cross bridge based on target of no sideslip," *Journal of PLA University of Science and Technology*, vol. 9, no. 4, pp. 373–377, 2008.
- [64] R. P. Marimuthu, B. C. Jang, and S. J. Hong, *A Study on SUV Parameters Sensitivity on Rollover Propensity*, SAE World Congress Detroit, Michigan, USA, 2006.
- [65] Z. S. Yu, *Automobile Theory*, China Machine Press, Beijing, China, 2011.
- [66] R. Lamm, B. Psarianos, and T. Mailaender, *Highway Design and Traffic Safety Engineering Handbook*, McGraw-Hill Companies, New York, 1999.
- [67] S. Dieter, H. Manfred, and B. Roberto, *Vehicle Dynamics: Modeling and Simulation (Germany)*, Springer-Verlag Berlin Heidelberg, Berlin, Germany, 2018.
- [68] Research Institute of Highway Ministry of Transport, *Inspection and Evaluation Quality Standards for Highway Engineering*, China, Beijing, 2004.
- [69] W. C. Liang and D. J. Cao, "Comparison study of three methods for road reconstruction based on matlab," *Agricultural Equipment & Vehicle Engineering*, vol. 51, no. 7, pp. 33–35, 2013.
- [70] K. M. Song, *Road Roughness Estimation Method Based on Vibration Test of Vehicle-Road Coupled System*, Harbin Institute of Technology, Haerbin, China, 2018.
- [71] Iso International Organization for Standardization, *Mechanical Vibration Road Surface Profiles - Reporting of Measured Data* International Standard ISO, Geneva, Switzerland, 2016.
- [72] G. Loprencipe and P. Zoccali, "Ride quality due to road surface irregularities: comparison of different methods applied on a set of real road profiles," *Coatings*, vol. 7, no. 5, 2017a.
- [73] G. Loprencipe and P. Zoccali, "Use of generated artificial road profiles in road roughness evaluation," *Journal of Modern Transportation*, vol. 25, no. 1, pp. 24–33, 2017b.
- [74] P. Zoccali and G. Cantisani, "Effects of vehicular speed on the assessment of pavement road roughness," *Applied Sciences*, vol. 9, no. 9, 2019.
- [75] Cccc First Highway Consultants Co., Ltd., *Design Specification for Highway Alignment*, People's Communications Press Co., Ltd, China, Beijing, 2017.
- [76] L. Y. Shan, X. S. Hou, and S. L. Ma, "Evaluation standard of pavement roughness based on ride comfort," *Journal of Harbin Institute of Technology*, vol. 40, no. 6, pp. 935–938, 2008.
- [77] X. M. Wang and B. B. Wang, "Expressway pavement power spectrum density," *Journal of Traffic and Transportation Engineering*, vol. 3, no. 2, pp. 53–56, 2003.
- [78] C. Q. Zhuang and C. X. He, *Fundamentals of Applied Mathematical Statistics*, South China University of Technology Press, Guangzhou, China, 4th edition, 2013.